Cell

Crosstalk between Muscularis Macrophages and Enteric Neurons Regulates Gastrointestinal Motility

Paul Andrew Muller,[1,2,3,10] Balázs Koscsó,[7] Gaurav Manohar Rajani,[7] Korey Stevanovic,[8] Marie-Luise Berres,[1,2,3] Daigo Hashimoto,[1,2,3,13] Arthur Mortha,[1,2,3] Marylene Leboeuf,[1,2,3] Xiu-Min Li,[5,6] Daniel Mucida,[10] E. Richard Stanley,[11] Stephanie Dahan,[3,4] Kara Gross Margolis,[8] Michael David Gershon,[9] Miriam Merad,[1,2,3,12,*] and Milena Bogunovic[1,2,3,7,12,*]

[1]Department of Oncological Sciences
[2]The Tisch Cancer Institute
[3]The Immunology Institute
[4]Division of Clinical Immunology, Department of Medicine
[5]Division of Allergy and Immunology, Department of Pediatrics
[6]Jaffe Food Allergy Institute
Icahn School of Medicine at Mount Sinai Hospital, New York, NY 10029, USA
[7]Department of Microbiology and Immunology, Penn State University College of Medicine and Milton Hershey Medical Center, Hershey, PA 17033, USA
[8]Department of Pediatrics, Morgan Stanley Children's Hospital
[9]Department of Pathology and Cell Biology
Columbia University College of Physicians and Surgeons, New York, NY 10032, USA
[10]Laboratory of Mucosal Immunology, The Rockefeller University, New York, NY 10065, USA
[11]Department of Developmental and Molecular Biology, Albert Einstein College of Medicine, Bronx, NY 10461, USA
[12]Co-senior author
[13]Present address: Department of Hematology, Hokkaido University Graduate School of Medicine, N15 W7, Kita-Ku, Sapporo 060-8638, Japan
*Correspondence: miriam.merad@mssm.edu (M.M.), mbogunovich@hmc.psu.edu (M.B.)
http://dx.doi.org/10.1016/j.cell.2014.04.050

SUMMARY

Intestinal peristalsis is a dynamic physiologic process influenced by dietary and microbial changes. It is tightly regulated by complex cellular interactions; however, our understanding of these controls is incomplete. A distinct population of macrophages is distributed in the intestinal muscularis externa. We demonstrate that, in the steady state, muscularis macrophages regulate peristaltic activity of the colon. They change the pattern of smooth muscle contractions by secreting bone morphogenetic protein 2 (BMP2), which activates BMP receptor (BMPR) expressed by enteric neurons. Enteric neurons, in turn, secrete colony stimulatory factor 1 (CSF1), a growth factor required for macrophage development. Finally, stimuli from microbial commensals regulate BMP2 expression by macrophages and CSF1 expression by enteric neurons. Our findings identify a plastic, microbiota-driven crosstalk between muscularis macrophages and enteric neurons that controls gastrointestinal motility.

INTRODUCTION

Peristaltic movements of the gut are essential to propel ingested material through the gastrointestinal (GI) tract. These movements are generated by coordinated contractions and relaxations of the circular and longitudinal smooth muscles that form the muscularis externa (Figure 1A). The pattern and frequency of peristaltic contractions are locally regulated by the enteric nervous system (ENS) (Furness, 2012) and pacemaker interstitial cells of Cajal (ICCs) (Huizinga et al., 1995; Rumessen and Vanderwinden, 2003).

Mononuclear phagocytes, which include dendritic cells (DCs) and macrophages, form a heterogeneous group of myeloid cells that are found in most tissues. Their common functions are to maintain tissue homeostasis through scavenging and participation in immune responses (Hashimoto et al., 2011b). A network of MHCII^{+} macrophages exists in the intestinal muscularis in both mice and humans (Mikkelsen and Rumessen, 1992; Mikkelsen et al., 1985). This network extends from the stomach to the distal colon (Mikkelsen, 2010). Within the muscularis, these macrophages mainly accumulate in layers, between the serosa and the longitudinal muscle, between longitudinal and circular muscles, and between the outer and inner circular muscles (Mikkelsen, 2010). In addition to their phagocytic properties (Mikkelsen et al., 1985), muscularis macrophages (MMs) are

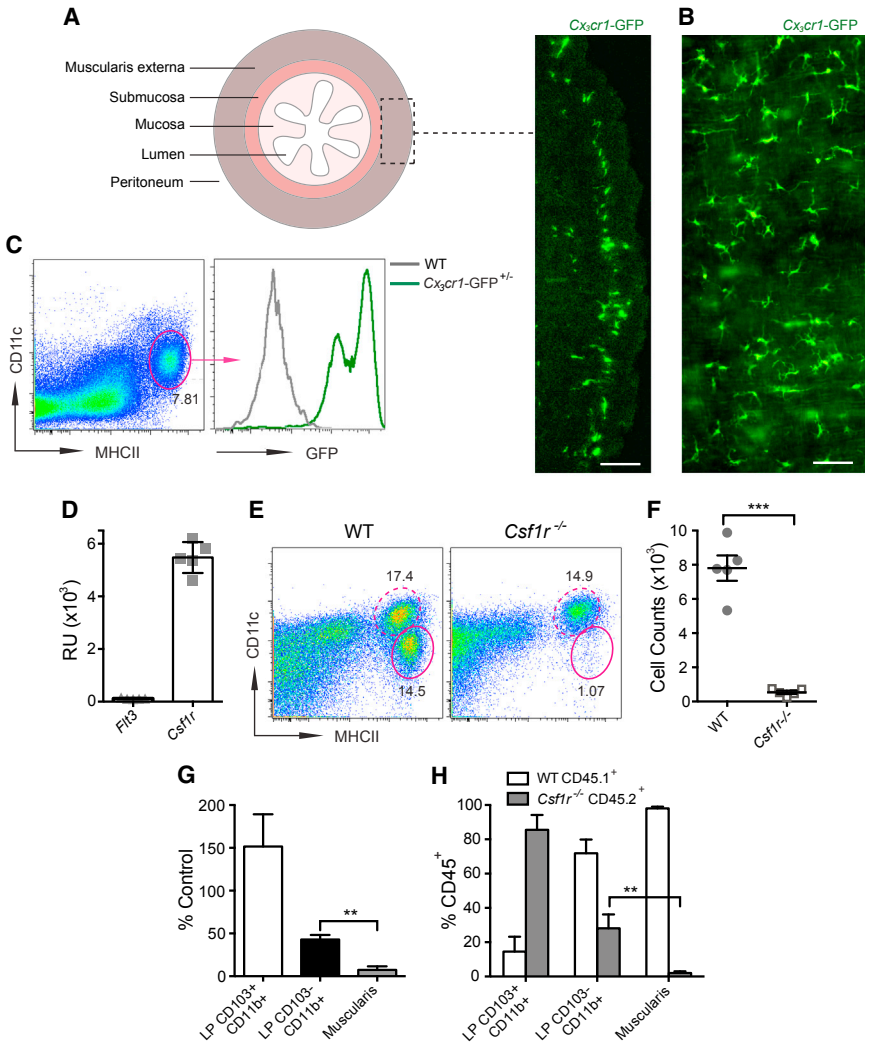

Figure 1. MHCII$^+$CX$_3$CR1$^+$ MMs Require CSF1R Signaling for Their Development

(A and B) Distribution of CX$_3$CR1$^+$ MMs shown in cross-section (A) and muscularis sheet (B) of LB from *Cx$_3$cr1*-GFP$^{+/-}$ mice. Scale bar, 100 nm.

(C) Phenotype of MMs in SB muscularis from *Cx$_3$cr1*-GFP$^{+/-}$ mice by fluorescence-activated cell sorting (FACS) analysis (gated on DAPI$^-$ cells).

(D) *Flt3* and *Csf1r* expression in sorted MMs measured by murine gene expression microarray and presented as relative units (RU). Data are presented as mean ± SEM.

(E) FACS plots of whole-bowel suspensions from WT or *Cscf1r*$^{-/-}$ mice show the percentage of CD11c^{lo}MHCII^{hi} MMs (oval gate, solid line) and CD11c^{hi}MHCII^{hi} LP phagocytes (oval gate, dashed line). Gated on CD45$^+$CD11c$^{lo/hi}$CD11b$^{lo/hi}$ cells as demonstrated in Figure S1.

(F) Absolute numbers of MMs in total gut of WT and *Csf1r*$^{-/-}$ mice quantified by FACS (mean ± SEM).

(G) Relative reduction of MMs and CD103$^+$CD11b$^+$ and CD103$^-$CD11b$^+$ LP phagocytes in *Csf1r*$^{-/-}$ mice as compared with WT littermates (quantified by FACS, mean ± SEM).

(H) Percentage of WT CD45.1$^+$ and *Csf1r*$^{-/-}$ CD45.2$^+$ cells among CD45$^+$ LP CD103$^+$CD11b$^+$ and LP CD103$^-$CD11b$^+$ phagocytes and MMs (muscularis) in SB from 10% WT + 90% *Csf1r*$^{-/-}$ mixed BM chimeras (mean ± SEM). See also Figure S1.

potent antigen-presenting cells and are sometimes referred to as DCs (Flores-Langarica et al., 2005).

The functions of MMs are far less defined compared to their mucosal counterparts. Some studies have implicated MMs in the pathogenesis of postoperative ileus, a transient inflammatory condition of the GI tract that results in intestinal paralysis (Mikkelsen, 2010). In surgically manipulated areas of the gut, the release of inflammatory mediators by activated MMs is thought to impair GI motility by affecting smooth muscle contractility directly, as well as through the recruitment of additional inflammatory cells (Boeckxstaens and de Jonge, 2009; Wehner et al., 2007). Whether MMs play a role in regulating constitutive GI physiology, however, has never been determined. Intrigued by the distinctive distribution of these cells and driven by the idea that macrophages are essential regulators of tissue homeostasis (Chow et al., 2011, 2013; Wynn et al., 2013), we hypothesized that MMs may provide trophic support to smooth muscle cells and, through that support, regulate constitutive GI motility.

To test our hypothesis, we developed a model for the selective transient depletion of MMs. We then demonstrated that MMs regulate intestinal peristalsis at steady state and identified a specific factor, BMP2, that is secreted by MMs and regulates GI motility through a direct action, not on smooth muscle, but on enteric neurons. Our work revealed that MMs and enteric neurons communicate with each other. MMs support enteric neurons by providing BMP2, whereas neurons promote MM homeostasis through production of the macrophage-specific growth factor CSF1. Finally, we have found that signals from the intestinal microbiota are able to influence the crosstalk between MMs and enteric neurons and alter GI motility.

RESULTS

MM Development Requires CSF1 Receptor Signaling

The intestine is a complex layered structure that includes the mucosa, submucosa, and muscularis externa (Figure 1A). The intestinal mucosa is populated by two prevalent subsets of mononuclear phagocytes (CD103$^+$CD11b$^+$CX$_3$CR1$^-$ DCs and CD103$^-$CD11b$^+$ CX$_3$CR1$^+$ macrophages), each with a different developmental pathway and function (Bogunovic et al., 2009, 2012). Very little is known about the phenotype and function of MMs, mainly because these cells are difficult to isolate from intestinal tissue. A technique for separating the intestinal muscularis externa from the overlying mucosa and submucosa allowed us to perform a detailed analysis of MMs using whole-mount tissue preparations and single-cell suspensions

(Bogunovic et al., 2009). By combining flow cytometry and immunofluorescence analysis, we showed that MMs represent a homogeneous population of MHCII^{hi}CD11c^{lo}CD103^{-}CD11b^{+} cells (Bogunovic et al., 2009) that express high levels of CX_3CR1 (Figures 1A–1C). The MM population resembles the CD103^{-}CD11b^{+}CX_3CR1^{+} macrophages, which are found in the intestinal lamina propria (LP) (Bogunovic et al., 2009). In a suspension of intestinal cells, MMs can easily be distinguished from CD11c^{hi} LP phagocytes by the lower expression of CD11c and higher expression of MHCII (Bogunovic et al., 2009; Figure S1A available online).

FLT3 and CSF1 (also known as macrophage colony stimulatory factor [M-CSF]) receptor (CSF1R) are two key growth factor receptors that control mononuclear phagocyte development (Hashimoto et al., 2011b). We previously demonstrated that CD103^{-}CD11b^{+} LP macrophages require CSF1R signaling for their homeostasis and are reduced in *Csf1r*$^{-/-}$ mice (Bogunovic et al., 2009). The phenotypic similarity between MMs and CD103^{-}CD11b^{+} LP macrophages led us to investigate the role of CSF1R in MM development. We found that MMs express *Csf1r* (Figure 1D) and must absolutely be dependent on CSF1R signaling because *Csf1r*$^{-/-}$ mice lack these cells (Figures 1E–1G). Moreover, *Csf1r*$^{-/-}$ bone marrow (BM) progenitors fail to develop into MMs when transplanted into lethally irradiated recipients (Figure 1H).

To study the function of MMs, we developed a model in which homeostatic properties are used to selectively deplete MMs. We found that MMs are more dependent on CSF1R signaling than LP phagocytes (Figures 1G and 1H), which provided us with a strategy to selectively deplete one population without affecting the other. Because CSF1R expression in the gut is restricted to MMs and mucosal macrophages (Figures S1B–S1D; small bowel (SB) mucosa and submucosa [data not shown]), a single intraperitoneal (i.p.) injection of a low dose of a blocking anti-CSF1R monoclonal antibody (Sudo et al., 1995) (αCSF1R mAb) was able to deplete at least 80% MMs (Figures 2A–2E, S2A, and S2B) without depleting LP phagocytes (Figures 2C, 2D, and S2B) or stromal cells (data not shown). MM numbers were reduced 24 hr after the antibody injection and returned to normal 7 days later (data not shown). No differences in CSF1R levels in MMs or MM depletion efficiency were observed between the SB and large bowel (LB) (Figures 2A–2E, S1C, S2A, and S2B). This depletion was considered to be noninflammatory because there was no lymphocyte (Figures 2F, S2C, and S2D), neutrophil, or monocyte (data not shown) recruitment in either the muscularis or mucosa. Injection of αCSF1R mAb also did not increase apoptotic cell numbers in the gut (Figure S2E). Taken together, these findings identified CSF1R as essential for MM development and established blocking CSF1R in vivo as a model for the transient depletion of these cells.

MMs Regulate GI Motility at Steady State

In the isolated intestine, one can elicit the peristaltic reflex by providing a distending force to the intestinal wall (Frigo and Lecchini, 1970). To determine whether conditional depletion of MMs affects the peristaltic reflex, we developed an ex vivo method to record peristaltic contractions in response to stepwise distension of colonic rings (Figure 3A). Repeated applications of increasing stretch resulted in an immediate contraction of the rings followed by gradual relaxation, creating a ladder-like pattern of recordings. Augmented stretching generated additional high-amplitude contractions (further called "stretch-induced contractions"), which gradually increased in amplitude and frequency (Figure 3B). In MM-depleted colonic rings, stretch-induced contractions were evoked at shorter durations of stretch, were more rapid, and had a significantly higher frequency (Figures 3B and 3C); thus the root-mean-square (rms) of the signal was increased (Figures 3C and 3D). Despite the evident colonic hyperreactivity ex vivo, colonic transit time, measured in vivo by bead expulsion assay, was increased after MM depletion, probably because the muscle contractions were poorly coordinated and inefficient (Figure 3E). Among other parameters of GI motility, gastric emptying was accelerated, whereas transit from the stomach along the SB and total intestinal transit time were not significantly changed (Figures S2F–S2H). This would occur if accelerated gastric emptying and delayed SB and LB motility cancel each other out, thus suggesting that the motility of the entire GI tract is affected by MM depletion.

To further confirm the role of MMs in regulating GI motility, we generated syngeneic BM chimeric animals with *Csf1r*$^{-/-}$ hematopoietic progenitors (from fetal liver). Some *Csf1r*$^{-/-}$ BM chimeric mice clearly developed a delay of colonic transit time (Figure S2I); however, poor engraftment of *Csf1r*$^{-/-}$ BM and the consequent low survival rate of these chimeric animals did not permit us to obtain enough animals for statistical comparisons.

In summary, the observation that removal of MMs results in dysmotility indicates that MMs contribute to the physiological regulation of GI motility.

MMs Regulate Intestinal Peristalsis through the Production of BMP2

These findings raised the question: by what mechanisms do MMs affect GI motility? We tested the initial hypothesis that MMs secrete a soluble factor that alters smooth muscle contractility. To identify the gene that encodes a putative target protein, we carried out a murine gene expression microarray on different purified intestinal phagocyte subsets (Bogunovic et al., 2009, 2012) and did a comparative data analysis to select genes that are highly expressed by MMs but not by related CD103^{-}CD11b^{+} LP macrophages. Bone morphogenetic protein 2 (BMP2) was identified as the only nonimmune gene among the "top four" most highly expressed genes that also encoded a soluble factor (*Cd163*, *F13a1*, *Clec4e*, and *Bmp2*; Figures 4A and 4B). No other BMP family members were expressed by either intestinal phagocyte subset (Figures 4C and results not shown). BMPs are a group of secreted proteins in the transforming growth factor β (TGF-β) superfamily that are thought to mainly control organ development (Hogan, 1996). *Bmp2*$^{-/-}$ mice are embryonically lethal (Zhang and Bradley, 1996) and *Bmp2*$^{+/-}$ mice are susceptible to hypoxic pulmonary hypertension characterized by sustained high pressure in pulmonary arteries due to increased vascular reactivity and structural remodeling (Anderson et al., 2010). BMP2 is highly expressed in the fetal (but not adult) gut, and BMP receptor (BMPR) signaling has been implicated in enteric smooth muscle and neuronal differentiation (Chalazonitis

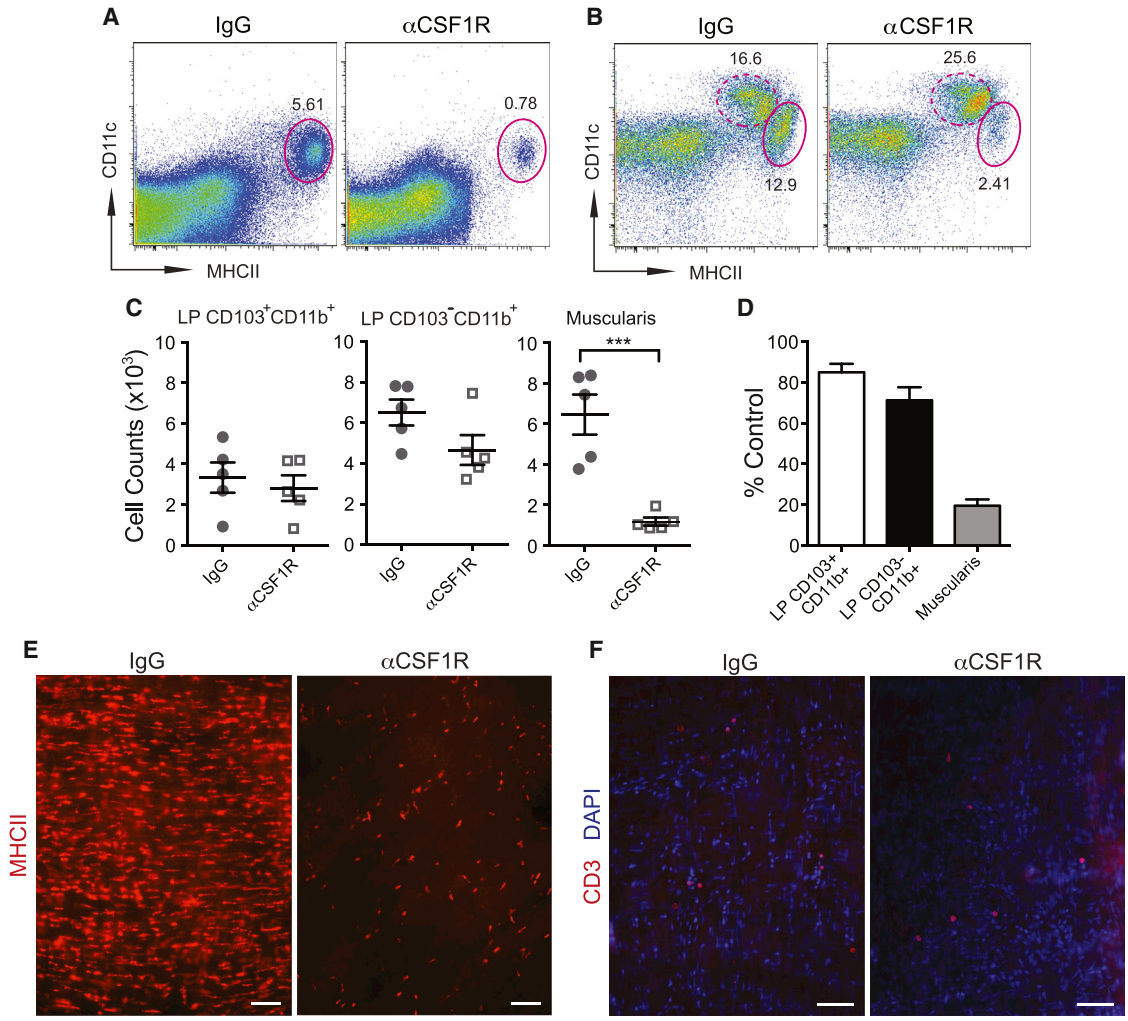

Figure 2. Model of MM Depletion

(A and B) FACS plots of separated SB muscularis (A) and whole SB (B) single-cell suspensions from WT mice 2 days after i.p. injection of isotype immunoglobulin G (IgG) or αCSF1R mAb show the percentage of CD11c^{lo}MHCII^{hi} MMs (oval gate, solid line) and CD11c^{hi}MHCII^{hi} LP phagocytes (oval gate, dashed line). (A) Gated on total viable cells. (B) Gated on CD45^{+}CD11c$^{lo/hi}$CD11b$^{lo/hi}$ cells using the gating strategy as in Figure S1.

(C) Absolute numbers of LP CD103^{+}CD11b^{+} and LP CD103^{-}CD11b^{+} phagocyte and MMs (muscularis) in the SB of WT mice 2 days after i.p. injection with isotype IgG or αCSF1R mAb quantified by FACS (mean ± SEM).

(D) Relative reduction of LP phagocyte and MM numbers quantified by FACS in WT mice treated with αCSF1R mAb (day 2) as compared with isotype IgG-treated mice (mean ± SEM).

(E and F) Distribution of MHCII^{+} macrophages (E) and CD3^{+} T cells (F) in LB muscularis from WT mice 2 days after i.p. injection of isotype IgG or αCSF1R mAb analyzed by immunofluorescence (IF). Scale bars, 100 nm.

See also Figure S2.

et al., 2004, 2008, 2011; Faure et al., 2007b; Fu et al., 2006; Goldstein et al., 2005). Using quantitative PCR (qPCR), we confirmed that *Bmp2* is expressed in MMs but is absent in purified muscularis lymphocytes (Figure 4D). In situ BMP2 protein expression was also restricted to MHCII^{+} MMs (Figure 4E). To examine whether BMP2 plays a role in regulating colonic motility, we compared the patterns of stretch-induced contraction of colonic rings in mice treated in vivo with the inhibitor of BMPR signaling, dorsomorphin (Yu et al., 2008), and mice treated only with vehicle. Treatment with dorsomorphin elicited a pattern of contractile hyperreactivity similar to that seen in colonic rings from MM-depleted mice (Figures 4F and S3A). To confirm that the pattern resulted from deficient BMPR signaling, we carried out a "rescue" experiment in which increasing concentrations of exogenous BMP2 were added to the colonic rings from MM-depleted mice. BMP2 was added during recording of stretch-induced contractions at a previously determined "optimal" 2.75 mm stretch distance. BMP2 reduced stretch-induced contractions in a concentration-dependent manner (Figures 4G–4I). There were no changes in contractility when the same amounts of BMP2 were added to colonic rings in which MMs had not been depleted (Figure 4G). Consistent with our in vitro data, BMP2

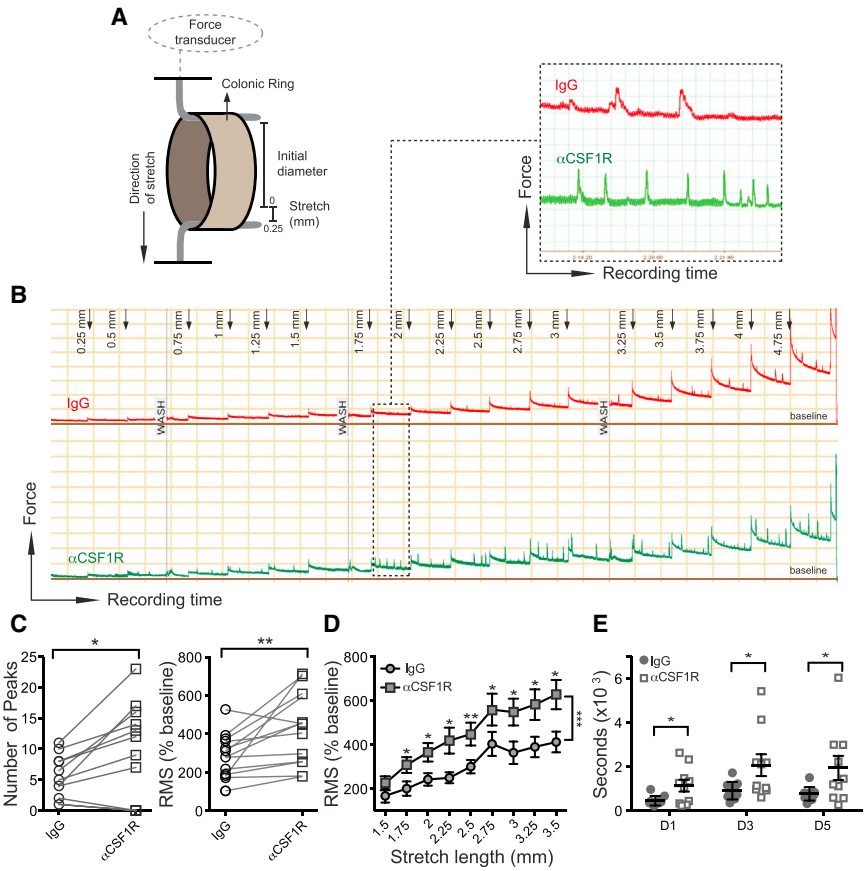

Figure 3. Depletion of MMs Results in Intestinal Dysmotility

(A) Illustration of the ex vivo method used to measure stretch-induced peristaltic contractions of colonic rings using a myograph.

(B) Five hour recording of stretch-induced contractions of colonic rings during repeated applications of 0.25-mm-long stretching up to 5.00 mm total stretch length; 3 mm colonic rings were obtained from WT mice 2 days after i.p. injection of isotype IgG or αCSF1R mAb.

(C) Number of peaks (left) and rms normalized to baseline in percent (right) during 10 min recordings of colonic contraction at a stretch distance of 2.75 mm.

(D) Rms normalized to baseline (%) during 10 min recordings of colonic contractions at each stretching step from 1.5 to 3.5 mm (mean ± SEM).

(E) Colonic transit time measured by bead expulsion assay in WT mice 1, 3, and 5 days after i.p. injection of isotype IgG or αCSF1R mAb (mean ± SEM).

See also Figure S2.

injection partially accelerated the colonic transit time (Figure 4J). Taken together, our data support the idea that MM secretion of BMP2 regulates colonic contractility.

MMs Activate Enteric Neurons that Express BMPR

We next sought to identify the cells targeted by MM-derived BMP2. The force with which smooth muscles contract in response to exogenous stimuli (stretch or KCl) was unaffected after MM depletion (Figures S3B and S3C). CKit$^+$ ICC and βIII-Tubulin$^+$ ENS networks do not overlap (Figure S4A). Both ICC and ENS networks remained intact after MP depletion (Figures 5C and S3D), indicating that acute MM depletion does not anatomically disrupt ICCs or the ENS. The numbers of epithelial serotonin$^+$ enteroendocrine cells, which activate peristaltic reflexes in response to luminal signals (Bulbring and Crema, 1959a, 1959b; Heredia et al., 2013), were also unaffected by injection of αCSF1R mAb (Figures S3E and S3F). Additionally, intestinal epithelial permeability remained unaffected even after treatment with maximal doses of αCSF1R mAb (Figures S3G and S3H). We assessed the anatomical interaction between MMs and enteric neurons and found that the vast majority of MMs were positioned along nerve fibers, often forming close appositions (Figure 5A). BMP2 signals through the oligomerization of type I and type II serine kinases (BMPRIa and BMPRII, respectively), which form BMPR (Kirsch et al., 2000). We found that BMPRII was selectively expressed by neurons marked by antibodies to βIII-Tubulin (Figure 5B), but not by ICCs (cKit$^+$; Figure S4B) or ENS-associated glia (GFAP$^+$; Figure S4C), suggesting that MMs act on enteric neurons. Ligand binding to BMPR activates the canonical signaling pathway through phosphorylation and nuclear translocation of SMADs 1, 5, and 8 (Derynck and Zhang, 2003). Treatment of cultured primary enteric neurons, which express *Bmprla* and *BmprII*, but not *Bmprlb* and *Bmp2* (Figure S4D), with recombinant BMP2 resulted in the rapid accumulation of pSMAD1/5/8 complex in the neuronal nuclei (Figure S4E). Moreover, the nuclei of the vast majority of BMPRII$^+$ enteric neurons in vivo were positive for pSMAD1/5/8, demonstrating that activation through BMPR was constitutively occurring (Figures 5C and 5D). In contrast, MM depletion resulted in the disappearance of pSMAD1/5/8 from nuclei in most of the enteric neurons in vivo, consistent with the key contribution of MMs to BMPR signaling (Figures 5C and 5D). Incubation of the muscularis layer devoid of MMs with exogenous BMP2 restored the numbers of enteric neurons with pSMAD1/5/8-immunoreactive nuclei to nearly normal levels (Figures 5C and 5D). These data imply that MMs provide continuous signaling to neurons through the secretion of BMP2, which activates the BMPR that they express.

Enteric Neurons Produce the Macrophage Growth Factor CSF1

CSF1 and interleukin-34 (IL-34) are two alternative ligands that activate CSF1R (Lin et al., 2008; Yeung et al., 1987) and each of these cytokines have been implicated in the development of different macrophage populations (Greter et al., 2012; Hashimoto et al., 2011b; Wang et al., 2012). MMs do not express either *Csf1* (Figure 1A) or *Il34* (data not shown), suggesting that CSF1 and IL-34 must be produced by a different cell

population, possibly stromal cells. CSF1 and Il-34 are alternatively expressed by distinct subtypes of mature neurons in the postnatal brain (Nandi et al., 2012). We thus asked whether there is additional crosstalk between enteric neurons and MMs in which enteric neurons provide CSF1R ligands to MMs. We found that enteric neurons express *Csf1*, but not *Il34* in culture (Figures 6A and 6B), and are the main source of CSF1 protein in the muscularis (Figure 6C). As expected, and consistent with an earlier report (Mikkelsen and Thuneberg, 1999), CSF1-deficient $Csf1^{op/op}$ mice almost completely lack MMs (Figures 6D–6F). These results suggest that enteric neurons likely play a key role in the maintenance of MM homeostasis.

Osteoclast-deficiency-related bone defects in $Csf1^{op/op}$ mice, including toothlessness (Wiktor-Jedrzejczak et al., 1991) and their significantly smaller size (Figure S5A), prevented us from analyzing GI motility in these animals. However, we observed that, despite the smaller size of both the length and diameter of the $Csf1^{op/op}$ intestine (length of SB: 80% of WT [Huynh et al., 2009]; length of LB: 80% of WT), the cecum of these animals was larger than of WT mice (Figure S5B), suggesting that GI motility is dysregulated in $Csf1^{op/op}$ mice. Consistent with our data obtained using the transient MM depletion model, we found that the numbers of $pSMAD1/5/8^{+}$ enteric neurons were significantly reduced in the colon of $Csf1^{op/op}$ mice compared with WT littermates (Figures 6G and S5C). We also observed a significant increase in the total numbers of enteric neurons together with a less organized architecture of the ENS in $Csf1^{op/op}$ mice (Figures 6H and 6I), suggesting the importance of MMs in ENS development. This observation is similar to previous findings regarding the ENS of NSE-noggin mice, which overexpress the endogenous BMP inhibitor noggin under the control of the neuron-specific enolase (NSE) promoter (Chalazonitis et al., 2004; Chalazonitis et al., 2008).

Luminal Microbiota Regulate Macrophage-Neuronal Crosstalk

Luminal microbiota appear to be essential for the normal regulation of intestinal motility, and severe dysmotility has been described in germ-free rodents (Abrams and Bishop, 1967; Gustafsson et al., 1970) and in $Tlr4^{-/-}$ and $Myd88^{-/-}$ mice (Anitha et al., 2012). The mechanisms by which commensals regulate intestinal motility are poorly understood and may involve abnormalities of many different cell types. Slowing of GI motility in germ-free, antibiotic-treated $Tlr4^{-/-}$ and $Myd88^{-/-}$ mice is accompanied by an alteration in the phenotypic diversity of enteric neurons with reduced numbers of nitrergic neurons (Anitha et al., 2012). Whether MMs contribute to these regulatory processes is not known. Similarly to published reports (Abrams and Bishop, 1967; Anitha et al., 2012; Gustafsson et al., 1970), we found that GI motility is grossly disturbed in mice treated with broad-spectrum antibiotics (Figures 7A, S6A, and S6B). Megacolon also occurs in these animals (Figure S7E), and thus a bead expulsion assay was not valuable for measuring colonic motility. Upon performing ex vivo analyses, we found that colonic rings from antibiotic-treated mice displayed a pattern of contractile hyperreactivity similar to that seen in colonic rings from MM-depleted or dorsomorphin-treated mice (Figures 7B and S6C). Strikingly, we found that antibiotic-treated mice expressed significantly less *Bmp2* compared with control mice (Figure 7C), suggesting that microbial commensals influence the interaction between MMs and enteric neurons. Consistently, the numbers of $pSMAD1/5/8^{+}$ enteric neurons were significantly reduced in antibiotic-treated mice compared with littermate controls that received only water (Figures 7D and S6D). We then questioned whether commensal signals can also regulate CSF1 production by enteric neurons. We found that addition of lipopolysaccharide (LPS) to cultured primary enteric neurons increased their expression of *Csf1* (Figure 7E), whereas culture of primary enteric neurons in the presence of exogenous BMP2 did not affect *Csf1* expression levels (data not shown). Consistently, antibiotic treatment in vivo reduced *Csf1* expression in the colonic muscularis (Figure 7F), although the kinetics of *Csf1* reduction was slow and reached its minimum after 4 weeks of treatment (Figure S7A). In line with the reduction of *Csf1*, antibiotic treatment also resulted in a decrease of MM numbers (Figures 7G, S7B, and S7C) with similar kinetics (Figure S7B). No reduction in the numbers of mucosal macrophages was observed during the course of antibiotic treatment (data not shown). Additionally, the numbers of $Gr1^{hi}$ blood monocytes that give rise to both mucosal macrophages (Bogunovic et al., 2009) and MMs (M.B., unpublished data) were not affected, thus excluding an effect on myeloid cell development in the BM (Figure S7D).

Microbiota-associated factors that influence GI motility include constituents of nutriment breakdown, byproducts of microbial metabolism, and microbial cellular components such as LPS (Reigstad and Kashyap, 2013). While cecum enlargement was an early sign of antibiotic treatment, cecum size continued to increase over the course of treatment (Figure S7E), implying that various microbiota-associated factors contribute to antibiotic-induced dysmotility with different kinetics. The kinetics of reduction in *Csf1* expression and MM numbers was delayed as compared with the reduction of bacteria in the gut lumen during the antibiotic treatment (Figure S7F), suggesting that a decrease in serum LPS after prolonged antibiotic treatment (Anitha et al., 2012) might be responsible for those changes. To test this, we supplemented mice with LPS in drinking water as described previously (Rakoff-Nahoum et al., 2004) while maintaining them on antibiotics. Consistent with the in vitro data and our hypothesis, LPS supplementation prevented the reduction of *Csf1* expression and MM numbers (Figures 7F, 7G, and S7C). LPS supplementation also partially improved GI transit time (Figure 7H) and reduced cecum size (Figure S7G).

Next, we asked whether the MM-neuronal crosstalk is reversible. Antibiotic-treated mice were reconstituted with microbiota following fecal transfer (FT) from untreated control mice. Repopulation of luminal bacteria to nearly normal levels (Figure S7H) was able to restore *Csf1* expression (Figure 7F) and MM numbers (Figure 7G) in the gut, and correct dysmotility (Figure 7I) and cecum size (Figure S7I).

Taken together, these results demonstrate that the function of both components of macrophage-neuronal crosstalk can be reversibly modified by luminal commensals.

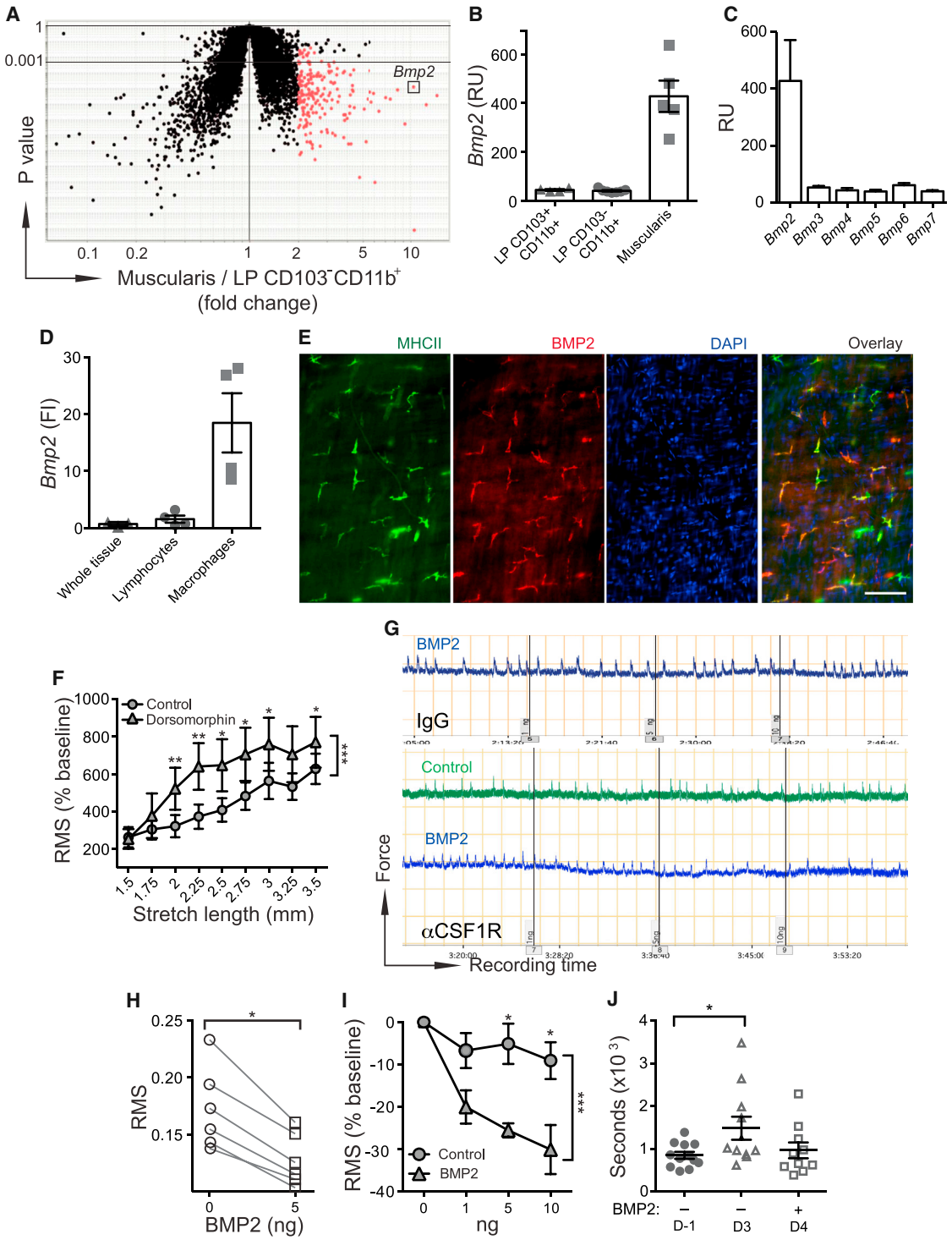

Figure 4. MMs Regulate Intestinal Peristalsis by Secreting BMP2

(A and B) *Bmp2* gene expression levels in MMs (muscularis) compared with LP CD103$^-$CD11b$^+$ phagocytes (A) and LP CD103$^+$CD11b$^+$ and LP CD103$^-$CD11b$^+$ phagocytes (B) measured by murine gene expression microarray (mean ± SEM).

(C) *Bmp2-7* gene-expression levels in MMs measured by murine gene expression microarray (mean ± SEM).

(D) *Bmp2* relative gene-expression levels measured by qPCR in intact SB muscularis (whole tissue) or in SSC^{lo}CD45$^+$CD11b$^-$ lymphocytes and macrophages sorted from separated SB muscularis. FI, fold increase as compared with "whole tissue" (mean ± SEM).

(E) IF analysis of LB muscularis from WT mice stained with anti-BMP2 and anti-MHCII mAbs and counterstained with DAPI. Scale bar, 100 nm.

(legend continued on next page)

DISCUSSION

MMs are thought to regulate GI motility during inflammation through secretion of inflammatory cytokines and the recruitment of inflammatory cells, which further accelerate the inflammatory process (Boeckxstaens and de Jonge, 2009; Mikkelsen, 2010; Wehner et al., 2007). This mechanism, however, has not been proven directly to occur. Our data demonstrate that MMs regulate GI motility even when the bowel is not inflamed, and MMs do so through production of the soluble growth factor BMP2. Whether BMP2 remains a key factor in regulating GI motility during inflammation remains to be determined.

Our study suggests that MM-derived BMP2 regulates the functional activity of neurons, transcending the known role of this growth factor in neuronal development (Chalazonitis et al., 2004, 2008). While MMs or MM-specific BMP2 may contribute to ENS development, as suggested by our data from *Csf1*$^{op/op}$ mice, the mechanisms by which BMPs affect homeostasis or the function(s) of differentiated enteric neurons are not clear. Studies of BMPR signaling in motoneurons at the neuromuscular junction of developing *Drosophila* larvae suggest that BMPR signaling regulates the microtubule stability of axons, fast axonal transport, and synaptic growth and stability (Aberle et al., 2002; Eaton and Davis, 2005; Eaton et al., 2002; Nahm et al., 2013; Wang et al., 2007). More recently, BMPs have been demonstrated to inhibit constitutive electrical activity in differentiating neurons of the developing *Xenopus* spinal cord (Swapna and Borodinsky, 2012). We postulate that BMPs may exert similar effects on adult neurons. It is also possible that additional MM-derived factors can affect the function of enteric neurons. A recent study revealed the role of the resident macrophages of the CNS, the microglia, in promoting learning-dependent synapse formation by providing brain-derived neurotrophic factor (BDNF) to neurons (Parkhurst et al., 2013). Likewise, macrophage populations at other sites may participate in regulating the physiology of organs through mechanisms similar to those observed in the gut and the brain.

The reduction of BMP2 expression in mice after antibiotic treatment implies that MMs are sensitive to changes in the luminal environment, but the mechanism of this sensitivity remains unknown. Interestingly, prolonged *Helicobacter hepaticus* infection has been shown to dramatically affect MM activation and behavior even though *Helicobacter* never crosses the epithelial barrier of the gut (Hoffman and Fleming, 2010). It appears plausible that alterations of MMs occur through a combination of downstream immune and neuronal surveillance in the mucosa, including signals provided by Toll-like-receptor-positive enteroendocrine cells (Bogunovic et al., 2007). It is also possible that MMs recognize commensal components directly by sensing systemic LPS found in the serum of normal mice (Anitha et al., 2012; Uramatsu et al., 2010).

Chronic disruption of normal peristaltic activity is a characteristic symptom of functional GI disorders such as irritable bowel syndrome (IBS). In IBS patients, dysmotility-related symptoms are often accompanied by symptoms associated with visceral hypersensitivity, an exaggerated perceptual response to peripheral stimuli that could result from altered processing of visceral neuronal afferent signals (Faure et al., 2007a). Histological analysis of full-thickness intestinal biopsies from IBS patients revealed signs of degenerative or inflammatory neuropathy (Lindberg et al., 2009; Törnblom et al., 2002). Changes in the microbial environment, such as a preceding bacterial GI infection and SB bacterial overgrowth, have been proposed to be causes of IBS (Peralta et al., 2009; Pimentel et al., 2000, 2002, 2003). An improved understanding of the interplay among enteric neurons, MMs, and luminal signals may thus provide new therapeutic strategies for the treatment and/or prevention of IBS.

EXPERIMENTAL PROCEDURES

Mice

All mice were housed in a specific pathogen-free environment at the Mount Sinai School of Medicine and Penn State College of Medicine and were used in accordance with protocols approved by the Institutional Animal Care and Utilization Committees. A list of the mouse strains used is provided in the Extended Experimental Procedures.

MP depletion was achieved by single i.p. injection of 37.5 μg/g αCSF1R mAb (clone AFS98; Sudo et al., 1995) purified from hybridomas as described previously (Hashimoto et al., 2011a).

Cell Isolation, Flow Cytometry, and Cell Sorting

Single-cell suspensions of intestinal muscularis externa or entire bowel were prepared, analyzed, and purified as described previously (Bogunovic et al., 2009).

Immunofluorescence

Separated intestinal muscularis externa or cultured enteric neurons were stained according to a previously described protocol (Bogunovic et al., 2009) with some modifications and using commercial reagents described in the Extended Experimental Procedures.

Gene Expression Microarray

A murine gene expression microarray was performed and normalized by the Immgen Project (http://www.immgen.org) as described previously (Miller et al., 2012). The gene-expression profile of MMs is posted on www.immgen.org under "Small intestine serosal macrophages," abbreviated as MF.CD11cloSer.SI.

(F) Rms of colonic contraction recordings normalized to baseline (%) at stretch intervals of 1.5–3.5 mm; 3 mm colonic rings were obtained from WT mice treated with the BMPR inhibitor dorsomorphin or control vehicle (mean ± SEM).

(G) WT mice were injected i.p. with isotype IgG (top) or αCSF1R mAb (bottom) and analyzed 2 days later. Panels show ex vivo recordings of stretch-induced contractions of colonic rings from these mice before and after adding 1, 5, or 10 ng of human recombinant BMP2 or control vehicle (performed at 2.75 mm "optimal" stretch distance).

(H) Rms of the 10 min recordings described in (G) (bottom: αCSF1R mAb-treated mice) before and after adding 5 ng of BMP2.

(I) Rms normalized to baseline (%) of recordings described in (G) (bottom: αCSF1R mAb-treated mice) after adding BMP2 (1, 5, or 10 ng) or control vehicle (mean ± SEM). Baseline here is the recording at the same stretch distance (2.75 mm) prior to adding BMP2 or control vehicle.

(J) Colonic transit time measured by bead expulsion assay in WT mice before they received αCSF1R mAb (day −1) and on days 3 and 4 after they received αCSF1R mAb; 18 and 3 hr before the last assessment (day 4), the mice received 1 μg of BMP2 i.p. (mean ± SEM).

See also Figure S3.

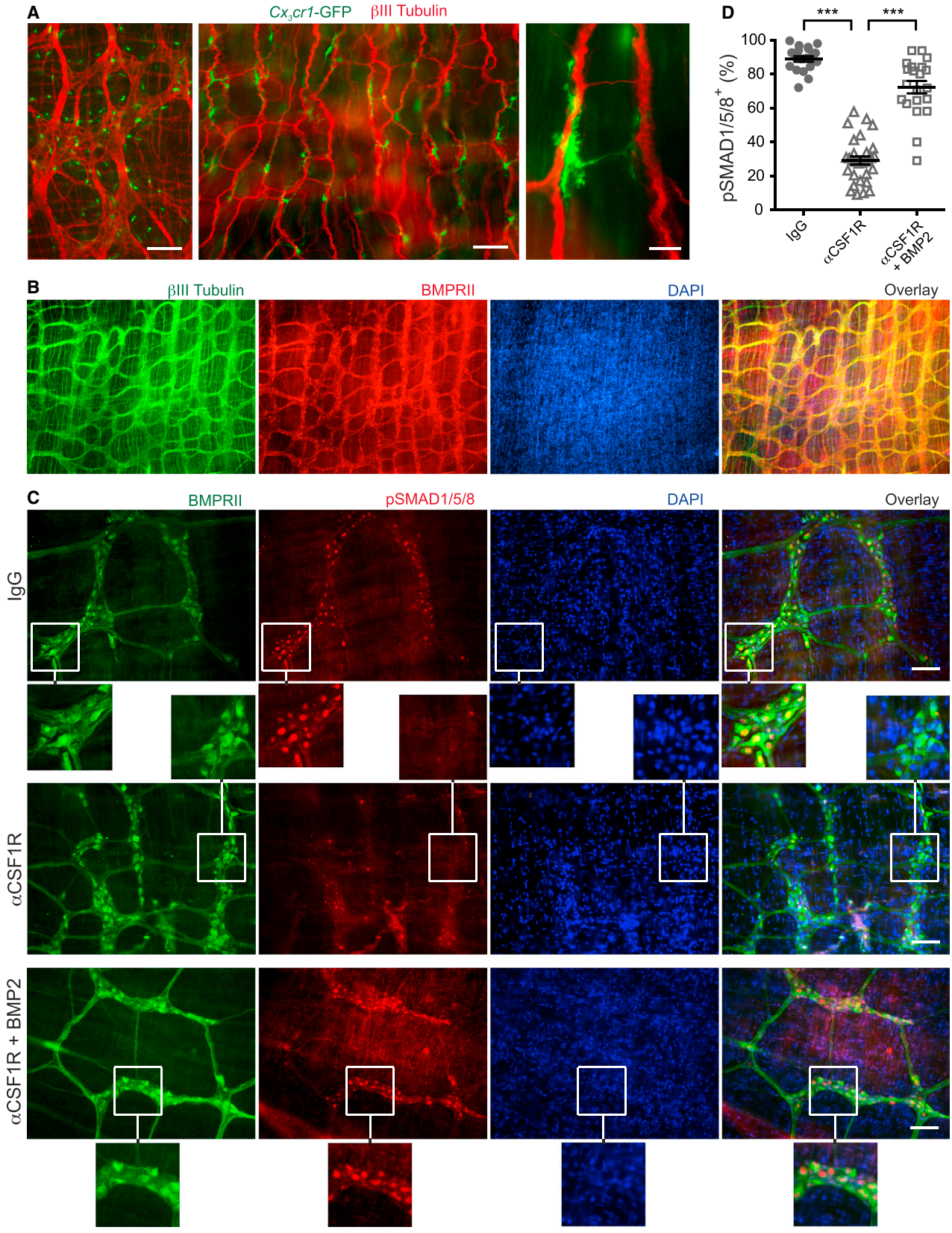

(legend on next page)

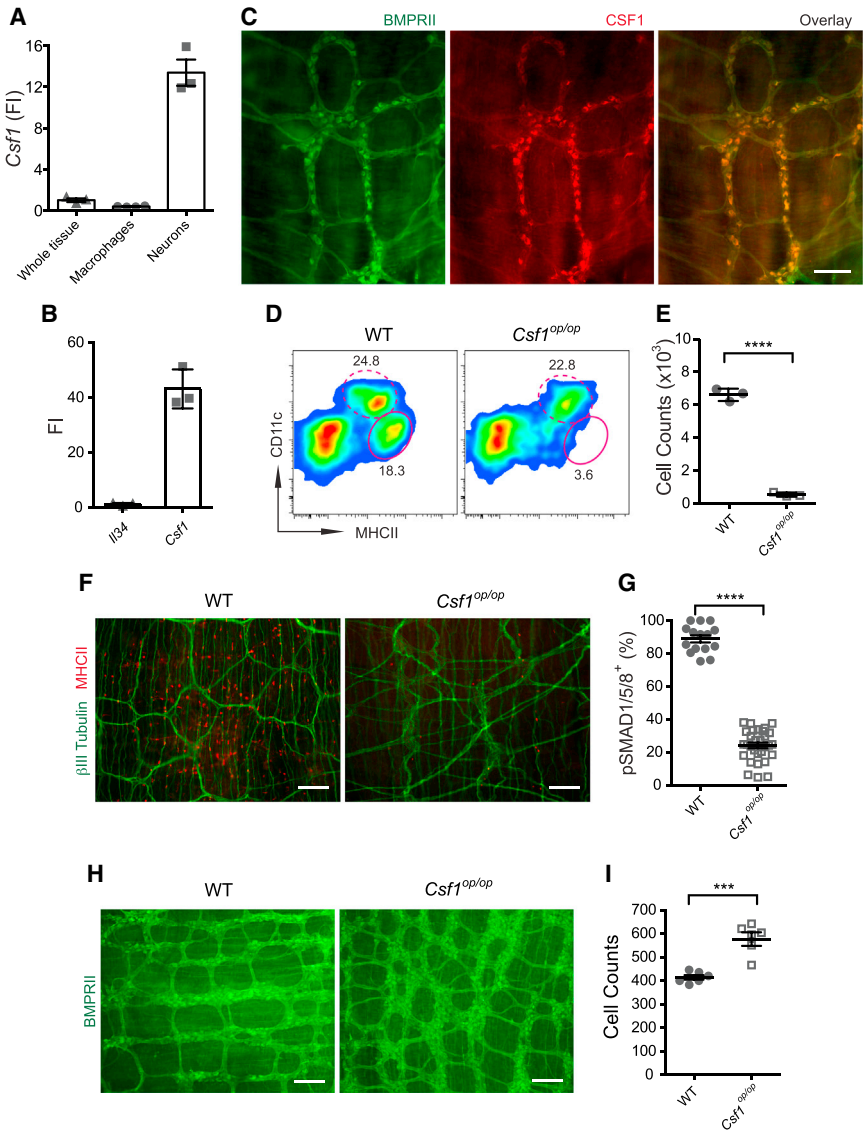

Figure 6. Enteric Neurons Produce CSF1 Required for MM Development

(A) *Csf1* gene-expression levels measured by qPCR in intact muscularis (whole tissue), macrophages sorted from SB muscularis, and cultured primary enteric neurons (FI compared with the "whole tissue"). Data are presented as mean ± SEM.

(B) *Il-34* and *Csf1* relative gene-expression levels (FI) measured by qPCR in cultured enteric neurons as compared with *Il-34* (mean ± SEM).

(C) IF analysis of LB muscularis from WT mice stained with anti-BMPRII and anti-CSF1 Abs. Scale bar, 100 nm.

(D) FACS plots of whole-bowel single-cell suspensions from WT mice and their $Csf1^{op/op}$ littermates show the percentage of $CD11c^{lo}MHCII^{hi}$ MMs (oval gate, solid line) and $CD11c^{hi}MHCII^{hi}$ LP phagocytes (oval gate, dashed line). Gated on $CD45^{+}CD11c^{lo/hi}CD11b^{lo/hi}$ cells.

(E) Absolute MM numbers in the bowels of WT mice and $Csf1^{op/op}$ mice quantified by FACS (mean ± SEM).

(F) IF analysis of LB (cecum) muscularis from WT mice and their $Csf1^{op/op}$ littermates stained with anti-βIII-Tubulin and anti-MHCII Abs. Scale bars, 500 nm.

(G) Quantitative summary of the distribution of $pSMAD1/5/8^{+}BMPRII^{+}$ neurons in the LB muscularis from WT and $Csf1^{op/op}$ mice. Each data point represents the percentage of $pSMAD1/5/8^{+}$ neurons among total $BMPRII^{+}$ neurons in each visual field; each column summarizes the results from three animals (mean ± SEM).

(H) IF analysis of LB (colon) muscularis from WT and $Csf1^{op/op}$ littermates stained with anti-BMPRII Ab. Scale bars, 500 nm.

(I) Quantitative summary of the distribution of $BMPRII^{+}$ neurons in the colon of WT and $Csf1^{op/op}$ mice. Each data point represents the counts of $BMPRII^{+}$ neurons in each visual field; each column summarizes the results from two animals.

See also Figure S5.

Real-Time PCR

Real-time PCR was performed as described previously (Bogunovic et al., 2009) with some modifications as explained in Extended Experimental Procedures. The data were normalized to β-actin. Each data dot on sorted primary cells was obtained by analyzing RNA from 50,000 cells purified from five to seven mice. Each data dot from cultured neurons was obtained by analyzing RNA from an independent primary neuronal culture.

Colonic Peristalsis Ex Vivo

The method used to measure colonic peristalsis ex vivo is described in the Extended Experimental Procedures. To block BMPR signaling, 13 mg/g (Helbing et al., 2011) of dorsomorphin (Sigma) in DMSO was injected i.p. 18 and 2 hr prior to analysis. In BMP2 "rescue" experiments the colonic rings were distended until 2.75 mm. A baseline recording of 40 min was taken, after which recombinant human BMP2 (R&D Systems) dissolved in 4 mM HCl was cumulatively added

Figure 5. MMs Activate BMP2 Receptor on Enteric Neurons

(A) Distribution of CX_3CR1^{+} MMs in colon (left) and ileum (middle and right) muscularis from Cx_3cr1-$GFP^{+/-}$ mice stained with anti-βIII-Tubulin Ab and analyzed by IF. Scale bars, 500 nm (left), 100 nm (middle), and 10 nm (right).

(B) IF analysis of LB muscularis from WT mice stained with anti-BMPRII and anti-βIII-Tubulin antibodies (Abs) and counterstained with DAPI. Scale bars, 500 nm.

(C) IF analysis of LB muscularis from WT mice 2 days after i.p. injection of isotype IgG (top) or αCSF1R mAb (middle and bottom), stained with anti-pSMAD1/5/8 and anti-BMPRII Abs and counterstained with DAPI. The bottom panel shows pSMAD1/5/8 distribution in the muscularis from an αCSF1R mAb-injected mouse that was incubated with BMP2 as described in (D). Scale bars, 100 nm.

(D) Quantitative summary of the distribution of $pSMAD1/5/8^{+}BMPRII^{+}$ neurons in the muscularis from WT mice 2 days after i.p. injection of isotype IgG or αCSF1R mAb. In all cases, the muscularis was incubated for 30 min at 37°C in complete medium in the presence or absence of BMP2 (10 ng/ml) as indicated. Each data point represents the percentage of $pSMAD1/5/8^{+}$ neurons among the total $BMPRII^{+}$ neurons in each visual field; each column summarizes the results from three animals (mean ± SEM).

See also Figures S3 and S4.

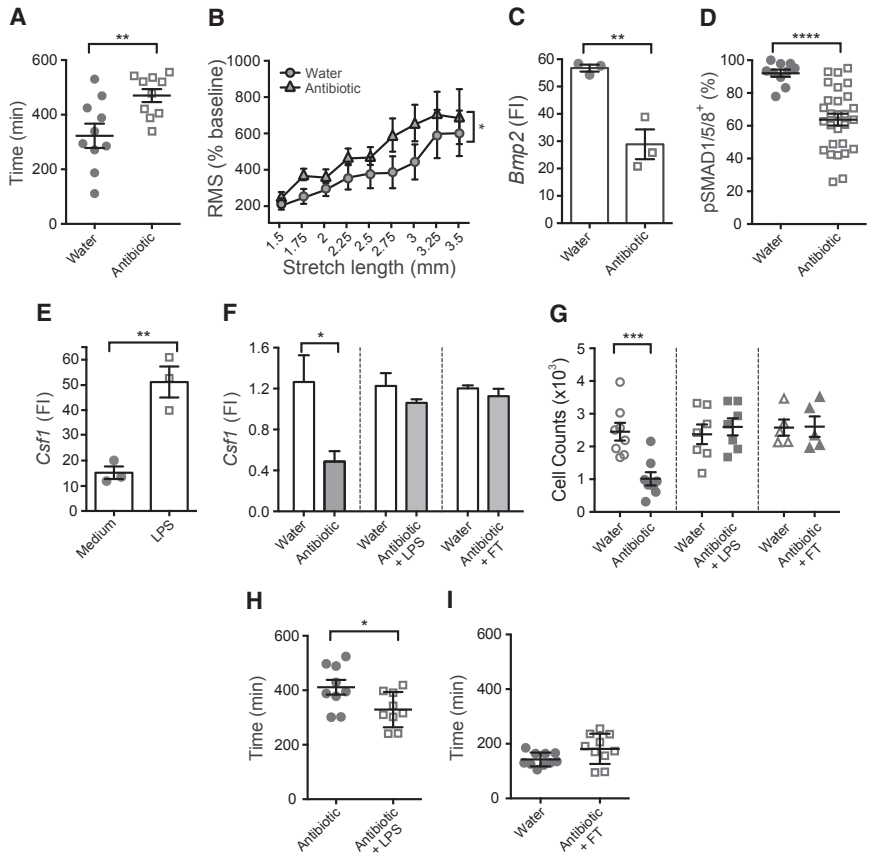

Figure 7. Luminal Microbiota Regulates Intestinal Motility and MM-Neuronal Cross-talk

(A–D) WT mice received antibiotics with drinking water for 4 weeks and control age-matched mice received only water.

(A) Total GI transit time, which represents the time required to expel feces containing carmine red dye, was measured in antibiotic-treated and control mice (mean ± SEM).

(B) Rms of colonic contraction recordings normalized to baseline (%) at stretch intervals of 1.5–3.5 mm (mean ± SEM); 3 mm colonic rings were obtained from antibiotic-treated and control mice.

(C) *Bmp2* relative gene-expression levels measured by qPCR in MMs sorted from SB muscularis of antibiotic-treated and control mice. FI, fold increase as compared with *Bmp2* levels in the intact muscularis (mean ± SEM). Each data point represents qPCR results obtained from analyzing 50,000 cells after a single sort from five mice. Cell sorting from each group was performed in pairs on the same day and under identical conditions.

(D) Quantitative summary of the distribution of pSMAD1/5/8^{+}BMPRII^{+} neurons in the muscularis from antibiotic-treated and control mice. Each data point represents the percentage of pSMAD1/5/8^{+} neurons among total BMPRII^{+} neurons in each visual field; each column summarizes the results from three animals (mean ± SEM).

(E) *Csf1* relative gene-expression levels in cultured primary enteric neurons measured by qPCR. Differentiated neurons were cultured with or without 10 ng/ml of LPS for 18 hr prior to analyses. FI, fold increase as compared with *Csf1* levels in the intact muscularis (mean ± SEM). Each data point represents qPCR results obtained from an independent neuronal culture.

(F) *Csf1* relative gene-expression levels quantified by qPCR in LB muscularis from WT mice treated with antibiotics for 4 weeks (left), WT mice treated with antibiotics and 50 μg/ml LPS in drinking water for 4 weeks (middle), and WT mice 3 weeks after they received fecal transfer (FT) following a 4-week course of antibiotics (right). The data are compared with data for age-matched control mice that received only water. FI, fold increase as compared with average *Csf1* levels in the control group that received water (mean ± SEM).

(G) Absolute numbers of MMs quantified by FACS in LB from WT mice that received antibiotics (left), antibiotics with LPS (middle), and FT following antibiotic treatment (right) as in (F). The data are compared with data for age-matched control mice that received only water (mean ± SEM).

(H) Total GI transit time in WT mice that received antibiotics and 50 μg/ml LPS with drinking water for 4 weeks and age-matched mice that received only antibiotics for 4 weeks (mean ± SEM).

(I) Total GI transit time in WT mice 3 weeks after they received FT following a 4-week course of antibiotics and control mice that received water (mean ± SEM). See also Figures S6 and S7.

to the bath (1, 5, and 10 ng per 8 ml organ bath) followed by 10 min of recording between doses. The dose response to KCl was determined by distending the colonic rings until a baseline force of 0.5 mN was achieved. The rings were allowed to equilibrate for 2.5 hr, with hourly solution changes. Increasing concentrations of KCl (0, 10, 40, 80, 100, and 200 mM) were added to the bath and solution was changed after 5 min. Ratios were calculated as baseline force prior to KCl addition over maximal contractile force after KCl addition.

GI Motility

Colonic transit time was detected by bead expulsion assay (Li et al., 2006). Gastric emptying, SB transit, and total intestinal transit time were measured as described previously (Li et al., 2011). Control and experimental groups were age and sex matched. For in vivo "rescue" experiments, human recombinant BMP2 (Peprotech) was injected i.p. (50 ng/g of body weight) 18 and 3 hr prior to measuring colonic transit time.

Epithelial Permeability

Epithelial permeability studies were performed as described previously (Dahan et al., 2011).

In Vitro Culture of Enteric Neurons

In vitro culture of enteric neurons was prepared from embryonic intestines from embryonic day 17 (E17) as described in Extended Experimental Procedures.

Antibiotic Treatment

For antibiotic treatment, a variation of a published protocol (Rakoff-Nahoum et al., 2004) was used. Six to 7-week-old female mice were given drinking water containing 1 g/l of ampicillin (Teknova), 1 g/l of streptomycin (GIBCO), 1 g/l of metronidazole (Sigma), and 1 g/l of vancomycin (Sigma) for 1–4 weeks. For LPS supplementation, mice were given 50 μg/ml of LPS from *E. coli* O111:B4 (Sigma) in drinking water (Rakoff-Nahoum et al., 2004) together with antibiotics for 4 weeks.

Fecal Transfer

Recipient mice were placed on antibiotic-free water 24 hr prior to FT. Intestinal contents from donor mice, prepared as described in Extended Experimental Procedures, were given to recipient mice by oral gavage. Donor mice were age matched, obtained from the same vendor, and maintained in the same facility as the recipients of FT.

Bacterial 16S rDNA qPCR

Bacterial 16S rDNA qPCR to quantify fecal bacterial DNA was performed as described in the Extended Experimental Procedures.

Statistical Analysis

Data are presented as mean ± SEM. The statistical significance of differences between group means was determined with the two-tailed unpaired or paired Student's t test and one-way ANOVA. Values of $p < 0.05$ (*), $p < 0.005$ (**), and $p < 0.0005$ (***) indicate statistical significance.

SUPPLEMENTAL INFORMATION

Supplemental Information includes Extended Experimental Procedures and seven figures and can be found with this article online at http://dx.doi.org/10.1016/j.cell.2014.04.050.

AUTHOR CONTRIBUTIONS

P.M. designed and performed experiments and helped to write the manuscript. M.B. led the project, designed and performed experiments, and wrote the manuscript. M.M. initiated and led the project and helped to write the manuscript. K.G.M. and M.D.G. provided intellectual input and helped to write the manuscript. D.M. and X.-M.L. assisted with methodology. E.R.S. provided reagents. B.K., G.R., K.S., S.D., M.-L.B., D.H., A.M., and M.L. performed experiments.

ACKNOWLEDGMENTS

We thank members of the Immgen Project (http://www.immgen.org) for performing a whole-mouse genome microarray and the Penn State Hershey Flow Cytometry Core Facility and the Mount Sinai Flow Cytometry Core for assistance with our experiments. We also thank Frederico Costa Pinta (Rockefeller University, New York, NY, and School of Veterinary Medicine, University of Sao Paulo, Brazil), Hongyan Zou (Icahn School of Medicine at Mount Sinai Hospital, New York, NY), and Florent Ginhoux (Singapore Immunology Network and Agency for Science, Technology and Research, Singapore) for productive discussions regarding the study, and Aron Lukacher (Penn State University College of Medicine, Hershey, PA) for help with the manuscript. This work was supported in part by grants from the NIH (AI09561, CA173861, and AI104848 to M.M.; CA32551 to E.R.S; and R21-AI105047 to D.M.), as well as a Career Development Award from the CCFA and PCARS from the NIAID (M.B.).

Received: June 26, 2013
Revised: December 12, 2013
Accepted: April 23, 2014
Published: July 17, 2014

REFERENCES

Aberle, H., Haghighi, A.P., Fetter, R.D., McCabe, B.D., Magalhães, T.R., and Goodman, C.S. (2002). wishful thinking encodes a BMP type II receptor that regulates synaptic growth in Drosophila. Neuron *33*, 545–558.

Abrams, G.D., and Bishop, J.E. (1967). Effect of the normal microbial flora on gastrointestinal motility. Proc. Soc. Exp. Biol. Med. *126*, 301–304.

Anderson, L., Lowery, J.W., Frank, D.B., Novitskaya, T., Jones, M., Mortlock, D.P., Chandler, R.L., and de Caestecker, M.P. (2010). Bmp2 and Bmp4 exert opposing effects in hypoxic pulmonary hypertension. Am. J. Physiol. Regul. Integr. Comp. Physiol. *298*, R833–R842.

Anitha, M., Vijay-Kumar, M., Sitaraman, S.V., Gewirtz, A.T., and Srinivasan, S. (2012). Gut microbial products regulate murine gastrointestinal motility via Toll-like receptor 4 signaling. Gastroenterology *143*, 1006–1016.e4.

Boeckxstaens, G.E., and de Jonge, W.J. (2009). Neuroimmune mechanisms in postoperative ileus. Gut *58*, 1300–1311.

Bogunovic, M., Davé, S.H., Tilstra, J.S., Chang, D.T., Harpaz, N., Xiong, H., Mayer, L.F., and Plevy, S.E. (2007). Enteroendocrine cells express functional Toll-like receptors. Am. J. Physiol. Gastrointest. Liver Physiol. *292*, G1770–G1783.

Bogunovic, M., Ginhoux, F., Helft, J., Shang, L., Hashimoto, D., Greter, M., Liu, K., Jakubzick, C., Ingersoll, M.A., Leboeuf, M., et al. (2009). Origin of the lamina propria dendritic cell network. Immunity *31*, 513–525.

Bogunovic, M., Mortha, A., Muller, P.A., and Merad, M. (2012). Mononuclear phagocyte diversity in the intestine. Immunol. Res. *54*, 37–49.

Bulbring, E., and Crema, A. (1959a). The action of 5-hydroxytryptamine, 5-hydroxytryptophan and reserpine on intestinal peristalsis in anaesthetized guinea-pigs. J. Physiol. *146*, 29–53.

Bulbring, E., and Crema, A. (1959b). The release of 5-hydroxytryptamine in relation to pressure exerted on the intestinal mucosa. J. Physiol. *146*, 18–28.

Chalazonitis, A., D'Autréaux, F., Guha, U., Pham, T.D., Faure, C., Chen, J.J., Roman, D., Kan, L., Rothman, T.P., Kessler, J.A., and Gershon, M.D. (2004). Bone morphogenetic protein-2 and -4 limit the number of enteric neurons but promote development of a TrkC-expressing neurotrophin-3-dependent subset. J. Neurosci. *24*, 4266–4282.

Chalazonitis, A., Pham, T.D., Li, Z., Roman, D., Guha, U., Gomes, W., Kan, L., Kessler, J.A., and Gershon, M.D. (2008). Bone morphogenetic protein regulation of enteric neuronal phenotypic diversity: relationship to timing of cell cycle exit. J. Comp. Neurol. *509*, 474–492.

Chalazonitis, A., D'Autréaux, F., Pham, T.D., Kessler, J.A., and Gershon, M.D. (2011). Bone morphogenetic proteins regulate enteric gliogenesis by modulating ErbB3 signaling. Dev. Biol. *350*, 64–79.

Chow, A., Lucas, D., Hidalgo, A., Méndez-Ferrer, S., Hashimoto, D., Scheiermann, C., Battista, M., Leboeuf, M., Prophete, C., van Rooijen, N., et al. (2011). Bone marrow CD169+ macrophages promote the retention of hematopoietic stem and progenitor cells in the mesenchymal stem cell niche. J. Exp. Med. *208*, 261–271.

Chow, A., Huggins, M., Ahmed, J., Hashimoto, D., Lucas, D., Kunisaki, Y., Pinho, S., Leboeuf, M., Noizat, C., van Rooijen, N., et al. (2013). $CD169^{+}$ macrophages provide a niche promoting erythropoiesis under homeostasis and stress. Nat. Med. *19*, 429–436.

Dahan, S., Rabinowitz, K.M., Martin, A.P., Berin, M.C., Unkeless, J.C., and Mayer, L. (2011). Notch-1 signaling regulates intestinal epithelial barrier function, through interaction with CD4+ T cells, in mice and humans. Gastroenterology *140*, 550–559.

Derynck, R., and Zhang, Y.E. (2003). Smad-dependent and Smad-independent pathways in TGF-beta family signalling. Nature *425*, 577–584.

Eaton, B.A., and Davis, G.W. (2005). LIM Kinase1 controls synaptic stability downstream of the type II BMP receptor. Neuron *47*, 695–708.

Eaton, B.A., Fetter, R.D., and Davis, G.W. (2002). Dynactin is necessary for synapse stabilization. Neuron *34*, 729–741.

Faure, C., Bouin, M., and Poitras, P. (2007a). Visceral hypersensitivity in irritable bowel syndrome: does it really normalize over time? Gastroenterology *132*, 464–465, author reply 465.

Faure, C., Chalazonitis, A., Rhéaume, C., Bouchard, G., Sampathkumar, S.G., Yarema, K.J., and Gershon, M.D. (2007b). Gangliogenesis in the enteric nervous system: roles of the polysialylation of the neural cell adhesion molecule and its regulation by bone morphogenetic protein-4. Dev. Dyn. *236*, 44–59.

Flores-Langarica, A., Meza-Perez, S., Calderon-Amador, J., Estrada-Garcia, T., Macpherson, G., Lebecque, S., Saeland, S., Steinman, R.M., and Flores-Romo, L. (2005). Network of dendritic cells within the muscular layer of the mouse intestine. Proc. Natl. Acad. Sci. USA *102*, 19039–19044.

Frigo, G.M., and Lecchini, S. (1970). An improved method for studying the peristaltic reflex in the isolated colon. Br. J. Pharmacol. *39*, 346–356.

Fu, M., Vohra, B.P., Wind, D., and Heuckeroth, R.O. (2006). BMP signaling regulates murine enteric nervous system precursor migration, neurite fasciculation, and patterning via altered Ncam1 polysialic acid addition. Dev. Biol. *299*, 137–150.

Furness, J.B. (2012). The enteric nervous system and neurogastroenterology. Nat. Rev. Gastroenterol. Hepatol. *9*, 286–294.

Goldstein, A.M., Brewer, K.C., Doyle, A.M., Nagy, N., and Roberts, D.J. (2005). BMP signaling is necessary for neural crest cell migration and ganglion formation in the enteric nervous system. Mech. Dev. *122*, 821–833.

Greter, M., Lelios, I., Pelczar, P., Hoeffel, G., Price, J., Leboeuf, M., Kündig, T.M., Frei, K., Ginhoux, F., Merad, M., and Becher, B. (2012). Stroma-derived interleukin-34 controls the development and maintenance of langerhans cells and the maintenance of microglia. Immunity *37*, 1050–1060.

Gustafsson, B.E., Midtvedt, T., and Strandberg, K. (1970). Effects of microbial contamination on the cecum enlargement of germfree rats. Scand. J. Gastroenterol. *5*, 309–314.

Hashimoto, D., Chow, A., Greter, M., Saenger, Y., Kwan, W.H., Leboeuf, M., Ginhoux, F., Ochando, J.C., Kunisaki, Y., van Rooijen, N., et al. (2011a). Pretransplant CSF-1 therapy expands recipient macrophages and ameliorates GVHD after allogeneic hematopoietic cell transplantation. J. Exp. Med. *208*, 1069–1082.

Hashimoto, D., Miller, J., and Merad, M. (2011b). Dendritic cell and macrophage heterogeneity in vivo. Immunity *35*, 323–335.

Helbing, T., Rothweiler, R., Ketterer, E., Goetz, L., Heinke, J., Grundmann, S., Duerschmied, D., Patterson, C., Bode, C., and Moser, M. (2011). BMP activity controlled by BMPER regulates the proinflammatory phenotype of endothelium. Blood *118*, 5040–5049.

Heredia, D.J., Gershon, M.D., Koh, S.D., Corrigan, R.D., Okamoto, T., and Smith, T.K. (2013). Important role of mucosal serotonin in colonic propulsion and peristaltic reflexes: in vitro analyses in mice lacking tryptophan hydroxylase 1. J. Physiol. *591*, 5939–5957.

Hoffman, S.M., and Fleming, S.D. (2010). Natural Helicobacter infection modulates mouse intestinal muscularis macrophage responses. Cell Biochem. Funct. *28*, 686–694.

Hogan, B.L. (1996). Bone morphogenetic proteins: multifunctional regulators of vertebrate development. Genes Dev. *10*, 1580–1594.

Huizinga, J.D., Thuneberg, L., Klüppel, M., Malysz, J., Mikkelsen, H.B., and Bernstein, A. (1995). W/kit gene required for interstitial cells of Cajal and for intestinal pacemaker activity. Nature *373*, 347–349.

Huynh, D., Dai, X.M., Nandi, S., Lightowler, S., Trivett, M., Chan, C.K., Bertoncello, I., Ramsay, R.G., and Stanley, E.R. (2009). Colony stimulating factor-1 dependence of paneth cell development in the mouse small intestine. Gastroenterology *137*, 136–144, e1–e3.

Kirsch, T., Nickel, J., and Sebald, W. (2000). BMP-2 antagonists emerge from alterations in the low-affinity binding epitope for receptor BMPR-II. EMBO J. *19*, 3314–3324.

Li, Z.S., Schmauss, C., Cuenca, A., Ratcliffe, E., and Gershon, M.D. (2006). Physiological modulation of intestinal motility by enteric dopaminergic neurons and the D2 receptor: analysis of dopamine receptor expression, location, development, and function in wild-type and knock-out mice. J. Neurosci. *26*, 2798–2807.

Li, Z., Chalazonitis, A., Huang, Y.Y., Mann, J.J., Margolis, K.G., Yang, Q.M., Kim, D.O., Côté, F., Mallet, J., and Gershon, M.D. (2011). Essential roles of enteric neuronal serotonin in gastrointestinal motility and the development/survival of enteric dopaminergic neurons. J. Neurosci. *31*, 8998–9009.

Lin, H., Lee, E., Hestir, K., Leo, C., Huang, M., Bosch, E., Halenbeck, R., Wu, G., Zhou, A., Behrens, D., et al. (2008). Discovery of a cytokine and its receptor by functional screening of the extracellular proteome. Science *320*, 807–811.

Lindberg, G., Törnblom, H., Iwarzon, M., Nyberg, B., Martin, J.E., and Veress, B. (2009). Full-thickness biopsy findings in chronic intestinal pseudo-obstruction and enteric dysmotility. Gut *58*, 1084–1090.

Mikkelsen, H.B. (2010). Interstitial cells of Cajal, macrophages and mast cells in the gut musculature: morphology, distribution, spatial and possible functional interactions. J. Cell. Mol. Med. *14*, 818–832.

Mikkelsen, H.B., and Rumessen, J.J. (1992). Characterization of macrophage-like cells in the external layers of human small and large intestine. Cell Tissue Res. *270*, 273–279.

Mikkelsen, H.B., and Thuneberg, L. (1999). Op/op mice defective in production of functional colony-stimulating factor-1 lack macrophages in muscularis externa of the small intestine. Cell Tissue Res. *295*, 485–493.

Mikkelsen, H.B., Thuneberg, L., Rumessen, J.J., and Thorball, N. (1985). Macrophage-like cells in the muscularis externa of mouse small intestine. Anat. Rec. *213*, 77–86.

Miller, J.C., Brown, B.D., Shay, T., Gautier, E.L., Jojic, V., Cohain, A., Pandey, G., Leboeuf, M., Elpek, K.G., Helft, J., et al.; Immunological Genome Consortium (2012). Deciphering the transcriptional network of the dendritic cell lineage. Nat. Immunol. *13*, 888–899.

Nahm, M., Lee, M.J., Parkinson, W., Lee, M., Kim, H., Kim, Y.J., Kim, S., Cho, Y.S., Min, B.M., Bae, Y.C., et al. (2013). Spartin regulates synaptic growth and neuronal survival by inhibiting BMP-mediated microtubule stabilization. Neuron *77*, 680–695.

Nandi, S., Gokhan, S., Dai, X.M., Wei, S., Enikolopov, G., Lin, H., Mehler, M.F., and Stanley, E.R. (2012). The CSF-1 receptor ligands IL-34 and CSF-1 exhibit distinct developmental brain expression patterns and regulate neural progenitor cell maintenance and maturation. Dev. Biol. *367*, 100–113.

Parkhurst, C.N., Yang, G., Ninan, I., Savas, J.N., Yates, J.R., 3rd, Lafaille, J.J., Hempstead, B.L., Littman, D.R., and Gan, W.B. (2013). Microglia promote learning-dependent synapse formation through brain-derived neurotrophic factor. Cell *155*, 1596–1609.

Peralta, S., Cottone, C., Doveri, T., Almasio, P.L., and Craxi, A. (2009). Small intestine bacterial overgrowth and irritable bowel syndrome-related symptoms: experience with Rifaximin. World J. Gastroenterol. *15*, 2628–2631.

Pimentel, M., Chow, E.J., and Lin, H.C. (2000). Eradication of small intestinal bacterial overgrowth reduces symptoms of irritable bowel syndrome. Am. J. Gastroenterol. *95*, 3503–3506.

Pimentel, M., Soffer, E.E., Chow, E.J., Kong, Y., and Lin, H.C. (2002). Lower frequency of MMC is found in IBS subjects with abnormal lactulose breath test, suggesting bacterial overgrowth. Dig. Dis. Sci. *47*, 2639–2643.

Pimentel, M., Chow, E.J., and Lin, H.C. (2003). Normalization of lactulose breath testing correlates with symptom improvement in irritable bowel syndrome. a double-blind, randomized, placebo-controlled study. Am. J. Gastroenterol. *98*, 412–419.

Rakoff-Nahoum, S., Paglino, J., Eslami-Varzaneh, F., Edberg, S., and Medzhitov, R. (2004). Recognition of commensal microflora by toll-like receptors is required for intestinal homeostasis. Cell *118*, 229–241.

Reigstad, C.S., and Kashyap, P.C. (2013). Beyond phylotyping: understanding the impact of gut microbiota on host biology. Neurogastroenterol. Motil. *25*, 358–372.

Rumessen, J.J., and Vanderwinden, J.M. (2003). Interstitial cells in the musculature of the gastrointestinal tract: Cajal and beyond. Int. Rev. Cytol. *229*, 115–208.

Sudo, T., Nishikawa, S., Ogawa, M., Kataoka, H., Ohno, N., Izawa, A., Hayashi, S., and Nishikawa, S. (1995). Functional hierarchy of c-kit and c-fms in intramarrow production of CFU-M. Oncogene *11*, 2469–2476.

Swapna, I., and Borodinsky, L.N. (2012). Interplay between electrical activity and bone morphogenetic protein signaling regulates spinal neuron differentiation. Proc. Natl. Acad. Sci. USA *109*, 16336–16341.

Törnblom, H., Lindberg, G., Nyberg, B., and Veress, B. (2002). Full-thickness biopsy of the jejunum reveals inflammation and enteric neuropathy in irritable bowel syndrome. Gastroenterology *123*, 1972–1979.

Uramatsu, M., Matsumoto, T., Tateda, K., Shibuya, K., Miyazaki, S., Horino, T., Tanabe, M., Sumiyama, Y., Kusachi, S., and Yamaguchi, K. (2010). Involvement of endotoxin in the mortality of mice with gut-derived sepsis due to methicillin-resistant Staphylococcus aureus. Microbiol. Immunol. *54*, 330–337.

Wang, X., Shaw, W.R., Tsang, H.T., Reid, E., and O'Kane, C.J. (2007). Drosophila spichthyin inhibits BMP signaling and regulates synaptic growth and axonal microtubules. Nat. Neurosci. *10*, 177–185.

Wang, Y., Szretter, K.J., Vermi, W., Gilfillan, S., Rossini, C., Cella, M., Barrow, A.D., Diamond, M.S., and Colonna, M. (2012). IL-34 is a tissue-restricted ligand

of CSF1R required for the development of Langerhans cells and microglia. Nat. Immunol. *13*, 753–760.

Wehner, S., Behrendt, F.F., Lyutenski, B.N., Lysson, M., Bauer, A.J., Hirner, A., and Kalff, J.C. (2007). Inhibition of macrophage function prevents intestinal inflammation and postoperative ileus in rodents. Gut *56*, 176–185.

Wiktor-Jedrzejczak, W., Urbanowska, E., Aukerman, S.L., Pollard, J.W., Stanley, E.R., Ralph, P., Ansari, A.A., Sell, K.W., and Szperl, M. (1991). Correction by CSF-1 of defects in the osteopetrotic op/op mouse suggests local, developmental, and humoral requirements for this growth factor. Exp. Hematol. *19*, 1049–1054.

Wynn, T.A., Chawla, A., and Pollard, J.W. (2013). Macrophage biology in development, homeostasis and disease. Nature *496*, 445–455.

Yeung, Y.G., Jubinsky, P.T., Sengupta, A., Yeung, D.C., and Stanley, E.R. (1987). Purification of the colony-stimulating factor 1 receptor and demonstration of its tyrosine kinase activity. Proc. Natl. Acad. Sci. USA *84*, 1268–1271.

Yu, P.B., Hong, C.C., Sachidanandan, C., Babitt, J.L., Deng, D.Y., Hoyng, S.A., Lin, H.Y., Bloch, K.D., and Peterson, R.T. (2008). Dorsomorphin inhibits BMP signals required for embryogenesis and iron metabolism. Nat. Chem. Biol. *4*, 33–41.

Zhang, H., and Bradley, A. (1996). Mice deficient for BMP2 are nonviable and have defects in amnion/chorion and cardiac development. Development *122*, 2977–2986.